Pre-print of: "Satellite data as indicators of tree biomass growth and forest dieback in a Mediterranean holm oak forest / R. Ogaya et al." In Annals of forest science (Springer), Jan.2015, vol. 72, no. 1, p. 135-144. DOI 10.1007/s13595-014-0408-y

Satellite data as indicators of tree biomass growth and forest dieback in a Mediterranean holm oak forest.

Abstract.

- Context: In the frame of climate change, decreased tree growth and enhanced mortality induced by hot and dry conditions are increasing in many forests around the world, and particularly in Mediterranean forests.
- Aims: Our aim was to estimate tree growth and mortality in a Mediterranean holm oak forest, using remote sensing data from MODIS.
- Methods: We monitored annual increases of aboveground biomass by measuring tree basal area, and we determined tree mortality by counting dead stems. We analyzed the relationships between forest growth and mortality with mean annual values of some MODIS products and meteorological data.
- Results: Mortality and increases of aboveground biomass correlated well with precipitation, September standardized precipitation/evapotranspiration indices (SPEI) and some MODIS products such as NDVI and enhanced vegetation index EVI. Other MODIS products such as gross primary production (GPP) and net photosynthesis, however, showed no clear relationship with tree mortality or measured increases of biomass.
- Conclusion: The MODIS products as proxies of ecosystemic productivity (gross primary productivity, net photosynthesis) were weakly correlated with biomass increase and did not reflect the mortality following the drought of autumn 2011. Nevertheless, NDVI and EVI were efficient indicators of forest productivity and dieback

Keywords: Forest productivity, Mediterranean forest, MODIS, remote sensing, SPEI indices, tree mortality.

Introduction.

Some forested ecosystems distributed in semi-arid and Mediterranean areas are seasonally exposed to water defficit and may be particularly vulnerable to even slight increases in water deficit, which can reduce tree growth (Barbeta et al. 2013; Ogaya and Peñuelas 2007), lower the condition of crowns (Carnicer et al. 2011; Galiano et al. 2012) and increase tree mortality (Allen et al. 2010; Breshears et al. 2005; Peng et al. 2011; Williams et al. 2012). Higher air temperatures are projected globally for the coming decades, and higher evapotranspiration rates induced by this increase in temperature and slight decreases in precipitation are expected in many areas, such as the Mediterranean Basin, subjected to seasonal drought (IPCC 2013). General circulation models project an average decrease of 15% in soil moisture over the next 50 years and a return period of extreme droughts 10 times shorter than in the twentieth century in these Mediterranean regions (Bates et al. 2008). Moreover, strong relationships between deficits in precipitation and subsequent occurrences of hot extremes have been widely observed (Mueller and Seneviratne 2012), and higher frequencies of heat waves coinciding with summer drought, higher evapotranspiration and the subsequent low availability of water are also expected for Mediterranean regions (Fischer and Schar, 2010).

Holm oak (*Quercus ilex* L.) is a widespread and dominant tree species in sub-humid areas of the Mediterranean Basin. Many tall shrub species with lower growth rates but a higher resistance to drought are associated with holm oak forests (Peñuelas et al. 1998; Ogaya and Peñuelas 2003). Under future drier conditions, higher mortality rates and lower seed production and seedling survival of *Q. ilex* could drive a decrease in the distribution of this dominant species and favor the associated species that are more resistant to a low availability of water (Lloret et al. 2004; Ogaya and Peñuelas 2007).

Monitoring the effects of climate change, particularly drought, on plant growth and mortality in various regions over time requires the use of remote-sensing techniques. Spectral indices from remote-sensing data are widely used to evaluate the structure and functioning of terrestrial ecosystems (Peñuelas and Filella 1998). The normalized difference vegetation index (NDVI), the most widely used remotely sensed index, is mainly used for estimating the fraction of the photosynthetically active radiation (FPAR) absorbed by the canopy (Tucker et al. 1985). The enhanced vegetation index (EVI) was developed to reduce the noise produced by soil background and atmospheric aerosols and to reduce the saturation of the reflectance signal at increasing levels of green biomass, which are commonly associated with the NDVI (Huete et al. 2002). Remote-sensing data can quantify the spatial variation in forest structure and growth (Waring et al. 2006) and stem volume (González Alonso et al. 2006). Both NDVI and EVI can provide good estimates of forest productivity but provide poor estimates of carbon uptake in dense evergreen forests such as those of the Mediterranean region, because these indices are largely insensitive to the short-term changes in CO_2 uptake that are caused by water defficit (Garbulsky et al. 2013).

The main objective of this work was to test the use of several MODIS products as tools for the detection and monitoring of biomass increase, forest decline and tree mortality in a typical Mediterranean forest and to assess the use of remote-sensing data from satellites as good indicators of forest productivity and dieback.

Material and methods.

Study site.

The study area was a valley (Vall dels Torners) in the Prades Mountains, Catalonia, in northeastern Spain (Fig. 1). This valley is populated by a natural holm oak (*Q. ilex* L.) forest (41º21' N, 1º2' E) at an altitude of 750-1050 m a.s.l. The soil is a Dystric Cambisol over Paleozoic schist, ranging in depth from 35 to 100 cm. The average annual temperature is 11.8 ºC, and the average annual rainfall is 659 mm (data from 1975 to 2012). Summer drought is pronounced and usually lasts for three months. The vegetation is a very dense multi-stem forest (16 616 stems ha^{-1}) dominated by *Q. ilex* L. (8633 stems ha^{-1}), *Phillyrea latifolia* L. (3600 stems ha^{-1}) and *Arbutus unedo* L. (2200 stems ha^{-1}), with an abundance of other evergreen species well adapted to dry conditions such as *Erica arborea* L., *Juniperus oxycedrus* L., *Cistus albidus* L. and occasional individuals of deciduous species such as *Sorbus torminalis* (L.) Crantz and *Acer monspessulanum* L. This forest has not been perturbed for 65 years, and the maximum height of the dominant species is approximately 6-10 m. Biomass increment and mortality rate of these species were annually measured as described in Barbeta et al. 2013, from 1999 to 2012.

Climate data.

An automated meteorological station installed at the study site has monitored temperature, photosynthetically active radiation, humidity and precipitation since late 1998. We estimated temperature and rainfall for years prior to 1998 with data from another meteorological station located at Poblet Monastery, 5.6 km northeast of our study area and at 510 m a.s.l. The meteorological data from the Poblet station was collected from late 1974 to July 2002, so we had climatic data for the period from August 1998 to July 2002 from both meteorological stations. We calculated the linear relationships between temperature (R^2=0.97) and rainfall (R^2=0.75) at these two stations for this period to estimate the climatic data at the study site from 1975. We thus had continuous climate data of the study site from 1975 to 2012.

Defoliation and mortality.

Defoliation and mortality were recorded in 2011. 40 dominant *Q. ilex* trees, 40 dominant *P. latifolia* and 40 dominant *A. unedo* shrubs were randomly selected across the study site in early spring 2011. The intensity of canopy defoliation by herbivores was estimated assessing the remaining petioles of consumed leaves at the end of July 2011. Canopy defoliation produced by summer drought conditions was thereafter estimated, in the same trees, assessing the brown color of dead leaves at the end of October 2011(Fig. 2). In both cases, we visually determined the percentage of defoliated or dead leaves in each tree, and later we calculated the mean value for all tree canopies. Eleven categories were established to measure the percentage of defoliation in each tree: 0%, 10%, 20%, 30%, 40%, 50%, 60%, 70%, 80%, 90% and 100% (mortality), as described in Ogaya and Peñuelas 2004.

Remote-sensing data.

Remote-sensing data from 2000 to 2012 were obtained from sensors of the Moderate Resolution Imaging Spectroradiometer (MODIS) onboard the Terra and Aqua satellites. The Terra satellite orbits Earth from north to south in the morning, and the Aqua satellite orbits from south to north in the afternoon. We used the normalized difference vegetation index (NDVI) and the enhanced vegetation index (EVI), obtained from the 16-day Terra MOD13Q1 and 16-day Aqua MYD13Q1 products, combined in series with 8-day data based on 20 selected 250 m x 250 m pixels. We selected the pixels across the distribution of holm oak forest in the valley (Fig. 1). We later calculated the mean values of the 20 selected pixels to estimate the average values of these indices for the entire holm oak forest in the valley.

We also used data for gross primary production (GPP) and net photosynthesis (PsnNet) obtained from the 8-day Terra MOD17A2 product, net primary production (NPP) obtained from the annual Terra MOD17A3 product, leaf area index (LAI) and FPAR obtained from the 8-day Aqua MYD15A2 product and the quotient (R_{858}/R_{1240}) between the reflectances at 858 nm (reference) and 1240 nm (water absorption) from the 8-day Terra MOD09A1 product. All MODIS products were collected from 2000 to 2010 from a 1 x 1 km pixel centered in the study area, except NDVI and EVI data, that were collected in the 20 selected 250 x 250 pixels. Mean annual values of the remotely sensed indices were calculated as annual integrations for each of the growing seasons covered by the NDVI, EVI, GPP, PsnNet, LAI, FPAR and R858/R1240 data, whereas NPP data were directly collected annually.

Data analysis.

The climate data (1975-2012) allowed us to calculate the standardized precipitation evapotranspiration index (SPEI) (Vicente-Serrano et al. 2010), an index based on the

149 difference between precipitation and potential evapotranspiration. Evapotranspiration
150 can be very important for determining variability in soil moisture, a key factor in plant-
151 water relations, The inclusion of potential evapotranspiration (PET) in the calculation of
152 the SPEI only affects the index when PET differs from average conditions, for example
153 under scenarios of global change (Vicente-Serrano et al. 2010). We selected September
154 SPEI indices for the comparison of the 2011 summer drought to those of previous years;
155 we used SPEI 3 and SPEI 6 indices (with data from three and six months before
156 September, respectively). We selected September SPEI 6 and December SPEI 12
157 indices for the statistical analyses of the other variables.

158 General linear models were constructed to examine the relationships of tree
159 mortality rates and increases in aboveground biomass with the changes of air
160 temperatures, rainfall and September SPEI 6 and December SPEI 12 indices during the
161 study period (1975-2012). Other general linear models examined the relationships of
162 tree mortality rates and increases in aboveground biomass with mean annual values of
163 NDVI, EVI, GPP, PsnNet and NPP. We have shown linear regressions because they
164 were the relationships that fit better with all the variables studied. All linear models
165 were constructed with the StatView software package (SAS Institute Inc., Cary, North
166 Carolina, USA).

167 Two redundancy analyses (RDAs) were performed to assess the relationships of
168 the physical data on biomass increase and tree mortality. This linear method was chosen
169 after performing a detrended correspondence analysis, which indicated that the length of
170 the gradient was short (Lepš and Šmilauer 2003). The physical variables were used as
171 *species* (*sensu* Canoco) and were centered and standardized, because the data differed in
172 scale of measurement. The significance of the first axis was tested using 499

permutations (Lepš and Šmilauer 2003). The biplots show the first two axes and are displayed with CanoDraw. Ordination was performed using Canoco for Windows 4.5.

Results.

Climate data.

Mean annual temperature ranged from 10.7 °C in 1984 to 13.1 °C in 2011, and total annual precipitation ranged from 376 mm in 2005 to 984 mm in 1996 (Fig. 3). During this period (1975-2012), mean annual air temperature increased by approximately 1.5 °C (R^2=0.42, P<0.001) (Fig. 3). This increase was due to the strong increases of 2.86 °C in spring and 2.22 °C in summer temperatures (R^2=0.58, P<0.001; and R^2=0.40, P<0.001, respectively) (P<0.001), while autumn and winter temperatures did not change. Precipitation, however, was quite variable, and annual precipitation decreased only slightly from 1975 to 2011 (Fig. 4). SPEI indices calculated in September were often negative during the later years, with a clear continuous decrease of both SPEI 3 and SPEI 6 indices since 1990 (Fig. 5). Both the September SPEI 3 and SPEI 6 indices were lowest in 2011, when high temperatures coincided with the maximum number of days with no rainfall (133 days with rainfall under 10 mm) and when tree mortality occurred.

Defoliation and mortality.

Q. ilex was the only species with significant defoliation by herbivores. For instance, there was a heavy infestation bythe caterpillar of the moth *Catocala nymphagoga* (Esp.) during late spring, that consumed an average 15% of *Q. ilex* leaves, all young leaves

198 just flushed in the previous one or two months. By the end of October 2011, just after
199 the long period of hot and dry conditions, *Q. ilex* trees had lost an average 14% of their
200 leaves, and few trees were completely defoliated and had dead stems. *Q. ilex* thus lost,
201 on average, 29% of their leaves. The other dominant species suffered less defoliation,
202 which was due only to drought: *A. unedo* shrubs lost approximately 6% of their leaves,
203 and *P. latifolia* shrubs lost only approximately 1% of their leaves.
204
205 *Remote sensing data.*
206 NDVI values showed an annual pattern with high values during winter, a decrease
207 during spring, the lowest values during late spring and early summer and a final
208 increase during late summer and autumn (Fig. 6). EVI values had an inverse annual
209 pattern, with maximum values during late spring and early summer and minimum
210 values during winter (Fig. 6).
211 The maximum mean annual NDVI (0.80) occurred in 2003, and the maximum
212 mean annual EVI (0.38) occurred in 2008, when annual precipitation was highest (926
213 mm in 2003 and 837 mm in 2008). The minimum mean annual NDVI and EVI (0.74
214 and 0.33, respectively) occurred in late autumn and winter 2011, during the period of
215 high tree mortality. NDVI values remained low during late 2011 and early 2012 and did
216 not exhibit the typical winter recovery. They began to increase slightly during spring
217 2012 and reached typical values only at the end of 2012 (Fig. 6). EVI values were low
218 during late 2011 and early 2012, as is usual during winter, but were lower than normal
219 after the drought of autumn 2011 and recovered to typical values during spring 2012
220 (Fig. 6). Increases in BAI and aboveground biomass correlated well with mean annual
221 NDVI and EVI values, the sum of spring and autumn mean temperatures, annual

222 precipitation, spring precipitation, the sum of spring and summer precipitation, and
223 September SPEI 6 and SPEI 12 indices (Table 1).

224 GPP and PsnNet values had a different annual pattern, with low values during
225 winter, maximum values during spring, a decrease during summer, another increase in
226 autumn (albeit with lower values than in spring) and a final decrease during late autumn
227 and winter (Fig. 7). GPP and PsnNet values in 2011 were higher than the mean values
228 of the period 2000-2010, except during the severe drought in September and October,
229 but GPP and PsnNet values completely recovered in late autumn (Fig. 7).

230 The canonical axis (RDA axis 1) explained 46.4% of the total variance in the
231 analysis of biomass increase, and the overall model was significant (P=0.01) (Fig. 8).
232 The canonical axis (RDA axis 1) explained 25.1% of the total variance in the analysis of
233 tree mortality, and the overall model was significant (P=0.01) (Fig. 9). As shown in
234 Figs. 8 and 9, a group of variables (NDVI, EVI, LAI, FPAR, R_{850}/R_{1240}, annual rainfall,
235 spring and spring-summer rainfall and September SPEI 6 and December SPEI 12
236 indices) correlated well with increases in aboveground biomass and with tree mortality
237 rates. In contrast, other variables (GPP, PsnNet and summer rainfall) were not clearly
238 correlated with increased biomass or tree mortality rates. Mean annual temperature was
239 negatively correlated with increased biomass and positively correlated with tree
240 mortality rates (Figs. 8 and 9).

241

242

243 **Discussion.**

244

245 The dry conditions increased stem mortality and decreased tree growth in the holm oak
246 forest (Barbeta et al. 2013; Ogaya and Peñuelas 2007). The constant increase in spring

and summer temperatures during 1975-2012 led to higher vapor-pressure deficits, and the September SPEI 3 and September SPEI 6 indices had negative values during the most recent years, particularly in September 2011. The atmospheric moisture demand is the primary mechanism by which high temperatures influence drought-sensitive tree populations (Liu et al. 2013), and this is consistent with our negative relationship between mean annual temperature and biomass increase and with our positive relationship between mean annual temperature and tree mortality rates. As expected, higher precipitation induced larger increases in biomass, with the exception of summer rainfall. The negative relationship between summer rainfall and increased biomass must be due to other climatic circumstances more conducive to tree growth, such as annual rainfall or September SPEI indices, because summer rainfall was always low.

The mortality of autumn 2011 coincided with a heavy infestation of *C. nymphagoga* during late spring 2011 that consumed a large proportion of recently flushed leaves. After recent droughts in Catalonia, particularly in summer 1994 when 80% of *Q. ilex* individuals in some areas had lost all their foliage (Lloret and Siscart 1995), a high percentage of *Q. ilex* trees resprouted from the base of the trunk, the upper branches of the canopy or both after the mortality induced by the extremely dry conditions (Espelta et al. 1999). The percentage of resprouting *Q. ilex* trees after the autumn 2011 mortality in our study forest, though, was negligible. The deterioration in the condition of the crown in *Q. ilex* soon after autumn 2011 was clearly associated with lower carbon reserves, and defoliated trees generally had less stored non-structural carbohydrates than did healthy trees (Rosas et al. 2013). For these reasons, carbon starvation induced by the continuous increase of temperatures during dry periods may be a key factor of forest dieback at our study site.

MODIS provides a large variety of remote sensing indices widely used in ecophysiological studies for determining plant activity and ecosystemic productivity (Peñuelas and Filella 1998). In our holm oak forest, the correlation between the R_{858}/R_{1240} ratio and biomass increase and the negative relationship with tree mortality rates may be due to the importance of water availability in determining tree growth in this Mediterranean ecosystem. Other indices such as LAI and FPAR were also positively correlated with biomass increase and negatively correlated with tree mortality, because FPAR depends on the total amount of leaves in the canopies. A decrease in the total amount of leaves remaining in the canopies of this forest was observed in *Q. ilex* under simulated drought conditions (Ogaya and Peñuelas 2006). NDVI and EVI indices were also well correlated with biomass increase, as has been observed in many other works (Gamon et al. 1995). High correlations between stem growth and EVI values have also been observed in this forest (Garbulsky et al. 2013). Despite their seasonal variability, the lowest NDVI and EVI values occurred in late autumn 2011 (when tree mortality occurred) and did not recover typical values until late spring 2012 (soon after the flush of new leaves), showing again that NDVI and EVI indices are good indicators of crown condition and forest dieback. In contrast, annual GPP, PsnNet and NPP values were poorly correlated with biomass increase or tree mortality rates, and seasonal GPP and PsnNet values did not significantly decrease during the period of tree mortality and subsequent months. This result was unexpected because these algorithms are specifically designed to directly estimate ecosystemic productivity.

In conclusion, the continuing increase of temperatures in this Mediterranean ecosystem has been correlated with lower growth rates and higher forest dieback. Some remote-sensing indices, such as NDVI and EVI, were good indices for estimating annual productivity and for determining the occurrence of forest dieback, whereas other

indices such as GPP, PsnNet and NPP were less useful for estimating productivity or for detecting tree mortality, at least in the holm oak forest studied.

Acknowledgments.

We are grateful to DARP (Generalitat de Catalunya), X. Buqueras and A. Vallvey for permission and assistance to conduct this research in the Poblet Holm Oak Forest.

Funding.

This research was financially supported by the Spanish Government projects **CGL2013-48074-P** and Consolider-Ingenio MONTES CSD2008-00040, by the Catalan government project **SGR2014-274** and by the ERC Synergy project SyG-2013-610028 IMBALANCE-P.

References.

Allen CD, Macalady AK, Chenchouni H, Bachelet D, McDowell N, Vennetier M, Kitzberger T, Rigling A, Breshears DD, Hogg EH, González P, Fensham R, Zhang Z, Castro J, Demidova N, Lim JH, Allard G, Running SW, Semerci A, Cobb N (2010) A global overview of drought and heat-induced tree mortality reveals emerging climate change risks for forests. Forest Ecol Manag 259:660-684.

Barbeta A, Ogaya R, Peñuelas J (2013) Dampening effects of long-term experimental drought on growth and mortality rates of a Holm oak forest. Global Change Biol In press.

Bates BC, Kundzewicz ZW, Wu S, Palutikof JP (2008) Climate Change and Water. Technical Paper of the Intergovernmental Panel on Climate Change. pp. 210.

Breshears DD, Cobb NS, Rich PM, Price KD, Allen CD, Balice RG, Romme WH, Kastens JH, Floyd ML, Belnap J, Anderson JJ, Myers OB, Meyer CW (2005) Regional vegetation die-off in response to global-change-type drought. Proc Natl Acad Sci USA 102:15144-15148.

345 Breshears DD, Myers OB, Meyer CW, Barnes FJ, Zou CB, Allen CD, McDowell NG,
346 Pokman WT (2009) Tree die-off in response to global change-type drought: mortality
347 insights froma decade of plant water potential measurements. Front Ecol Environ 7:185-
348 189.
349
350 Carnicer J, Coll M, Ninyerola M, Pons X, Sanchez G, Peñuelas J (2011) Widespread
351 crown condition decline, food web disruption, and amplified tree mortality with
352 increased climate change-type drought. Proc Natl Acad Sci USA 108: 1474-1478.
353
354 CREAF (2009) Land Cover Map of Catalonia (MCSC), 4th Edition.
355 http://www.creaf.uab.es/mcsc/usa/index.htm. Accessed 23 September 2009
356
357 Espelta JM, Sabaté S, Retana J (1999) Resprouting dynamics. In: Rodà F, Retana J,
358 Gracia C, Bellot J (eds) Ecology of Mediterranean evergreen oak forests. Springer,
359 Berlin, pp 61-73
360
361 Fischer EM, Schar C (2010) Consistent geographical patterns of changes in high-impact
362 European heatwaves. Nature Geosc 3:398-403
363
364 Galiano L, Martinez-Vilalta J, Sabate S, Lloret F (2012) Determinants of drought
365 effects on crown condition and their relationship with depletion of carbon reserves in a
366 Mediterranean holm oak forest. Tree Physiol 32:478-489.
367

368 Gamon JA, Field CB, Goulden M, Griffin K, Hartley A, Joel G, Peñuelas J, Valentini, R
369 (1995) Relationships between NDVI, canopy structure, and photosynthetic activity in
370 three Californian vegetation types. Ecol Appl 5:28-41.
371
372 Garbulsky M, Peñuelas J, Ogaya R, Filella (2013) Leaf and stand-level carbon uptake of
373 a Mediterranean estimated using the satellite-derived reflectance indices EVI and PRI.
374 Int J Remote Sens 34:1282-1296.
375
376 Huete A, Didan K, Miura T, Rodriguez EP, Gao X, Ferreira LG (2002) Overview of the
377 radiometric and biophysical performance of the MODIS vegetation indices. Remote
378 Sens Environ 83:195-213.
379
380 IPCC (2013) Climate change 2013: The physical Science Basis. Contribution of
381 Working Group I to the Fifth Assessment Report of the Intergovernmental Panel on
382 Climate Change. In: Stocker TF, Qin D, Plattner GK, Tignor MMB, Allen SK,
383 Boschung J, Nauels A, Xia Y, Bex V, Midgley PM (eds) Cambridge University Press,
384 Cambridge, United Kingdom and New York, NY, USA. pp 986.
385
386 Lepš J, Šmilauer P (2003) Multivariate analysis of ecological data using CANOCO.
387 Cambridge Univ. Press, Cambridge.
388
389 Liu H, Williams AP, Allen CD, Guo D, Wu X, Anenkhonov OA, Liang E, Sandanov
390 DV, Yin Y, Qi Z, Badmaeva NK (2013) Rapid warming accelerates tree growth decline
391 in semi-arid forests of Inner Asia. Global Change Biol19: 2500-2510.
392

393 Lloret F, Siscart D (1995) Demographic drought effects on holm oak populations. Cuad
394 Soc Esp Cien Forest 2:77-81.
395
396 Lloret F, Peñuelas J, Ogaya (2004) Establishment of co-existing Mediterranean tree
397 species under a varying soil moisture regime. J Veg Sci 15:237-244.
398
399 Mueller B, Seneviratne S (2012) Hot days induced by precipitation deficits at the global
400 scale. Proc Natl Acad Sci USA 109: 12398-12403.
401
402 Ogaya R, Peñuelas J (2003) Comparative seasonal gas exchange and chlorophyll
403 fluorescence of two dominant woody species in a Holm Oak forest. Flora 198: 132-141.
404
405 Ogaya R, Peñuelas J. 2004. Phenological patterns of *Quercus ilex*, *Phyllirea latifolia*,
406 and *Arbutus unedo* growing under a field experimental drought. Écoscience 11: 263-270.
407
408 Ogaya R, Peñuelas J (2006) Contrasting foliar responses to drought in *Quercus ilex* and
409 *Phillyrea latifolia*. Biol Plantarum 50: 373-382.
410
411 Ogaya R, Peñuelas J (2007) Tree growth, mortality, and above-ground biomass
412 accumulation in a holm oak forest under a five-year experimental field drought. Plant
413 Ecol 189: 291-299.
414
415 Peng C, Ma Z, Lei X (2011) A drought-induced pervasive increase in tree mortality
416 across Canada's boreal forests. Nature Clim Change. DOI: 10.1038/nclimate1293.
417

418 Peñuelas J, Filella I, Llusià J, Siscart D, Piñol J (1998) Comparative field study of
419 spring and summer leaf gas Exchange and photobiology of the Mediterranean trees
420 *Quercus ilex* and *Phillyrea latifolia*. J Exp Bot 49: 229-238.
421
422 Peñuelas J, Filella I (1998) Visible and near-infrared reflectance techniques for
423 diagnosing plant physiological status. Trends Plant Sci 3: 151-156.
424
425 Rosas T, Martínez-Vilalta J, Galiano L (2013) Non-structural carbohydrates in three
426 Mediterranean woody species are unaffected by long-term experimental drought.
427 Submitted.
428
429 Tucker CJ, Vanpraet CL, Sharman MJ, Vanittersum G (1985) Satellite Remote-Sensing
430 of Total Herbaceous Biomass Production in the Senegalese Sahel - 1980-1984. Remote
431 Sens Environ 17: 233-249.
432
433 Vicente-Serrano SM, Begueria S, Lopez-Moreno JI (2010) A Multiscalar Drought
434 Index Sensitive to Global Warming: The Standardized Precipitation Evapotranspiration
435 Index. J Climate 23: 1696-1718.
436
437 Williams AP, Allen CD, Macalady AK, Griffin D, Woodhouse CA, Meko DM,
438 Swetnam TW, Rauscher SA, Seager R, Grissino-Mayer HD, Dean JS, Cook ER,
439 Gangodagamage C, Cai M, McDowell NG (2012) Temperature as a potent driver of
440 regional forest drought stress and tree mortality. Nature Clim Change. DOI:
441 10.1038/nclimate1693.
442

Tables.

Table 1. Coefficients of determination (R^2) of the linear relationships of biomass increase and mortality with spectral indices and meteorological variables. (N.S. means not significant).

	Biomass Increase	Mortality
NDVI	0.64	0.43
EVI	0.55	0.35
GPP	N.S.	N.S.
PsnNet	N.S.	N.S.
Annual precipitation	0.53	0.24
Spring precipitation	0.44	0.31
Spring + Summmer precipitation	0.41	0.34
Mean annual temperature	N.S.	0.33
Spring + Autumn temperature	0.16	0.38
September SPEI 6	0.30	0.31
December SPEI 12	0.45	0.27

Figure captions.

Figure 1. Study site with the land-cover types obtained from the "Land Cover Map of Catalonia" (CREAF 2009) (modified legend). The study site is depicted by a red square in the map of Europe. The 20 selected pixels of NDVI and EVI values are framed in black. The other values were calculated in 1 x 1 km pixel, centered in the middle of these pixels, and covering the area of 16 depicted pixels.

Figure 2. Photographs showing the mortality in the studied forest during early autumn 2011 and the same forest with healthy trees in autumn 2010.

Figure 3. Mean annual temperature and annual precipitation at the study site. The straight lines represent the linear relationships of an increase of air temperatures and a decrease of rainfall during the 36 years that meteorological data were collected. N.S. means not significant. Each point indicates the mean value of 1 year.

Figure 4. Monthly data of air temperatures and precipitation during 2011 (black points) compared to the average data during 1975-2010 (white points and grey columns). Each point and column indicates the mean value of 1 month. Error bars indicate the standard errors of the means for 1975-2010.

Figure 5. Values of September standardized precipitation evapotranspiration index (SPEI) for 1975-2012. SPEI 3 is calculated with meteorological data during the three months before September (included), and SPEI 6 is calculated with data during the six months before September (included).

Figure 6. Monthly variations of the normalized difference vegetation index (NDVI) and the enhanced vegetation index (EVI) in 2011 and 2012 (black points) compared to the average of 2000-2010 (white points). Each point indicates the mean value of 1 month. Error bars indicate the standard errors of the means for 2000-2010.

Figure 7. Monthly variations of gross primary production (GPP) and net photosynthesis (PsnNet)in 2011 (black points) compared to the average of 2000-2010 (white points). Error bars indicate the standard errors of the means for 2000-2010.

Figure 8. RDA biplot representing the relationships of the physical data on biomass increase. Abbreviations: “temp” is mean annual temperature, “spring-summer” is the sum of spring and summer rainfall and “SPEI 6” and “SPEI 12” are the September SPEI 6 and December SPEI 12 indices, respectively.

Figure 9. RDA biplot representing the relationships of the physical data on mortality. Abbreviations: “temp” is mean annual temperature, “spring-summer” is the sum of spring and summer rainfall and “SPEI 6” and “SPEI 12” are the September SPEI 6 and December SPEI 12 indices, respectively.

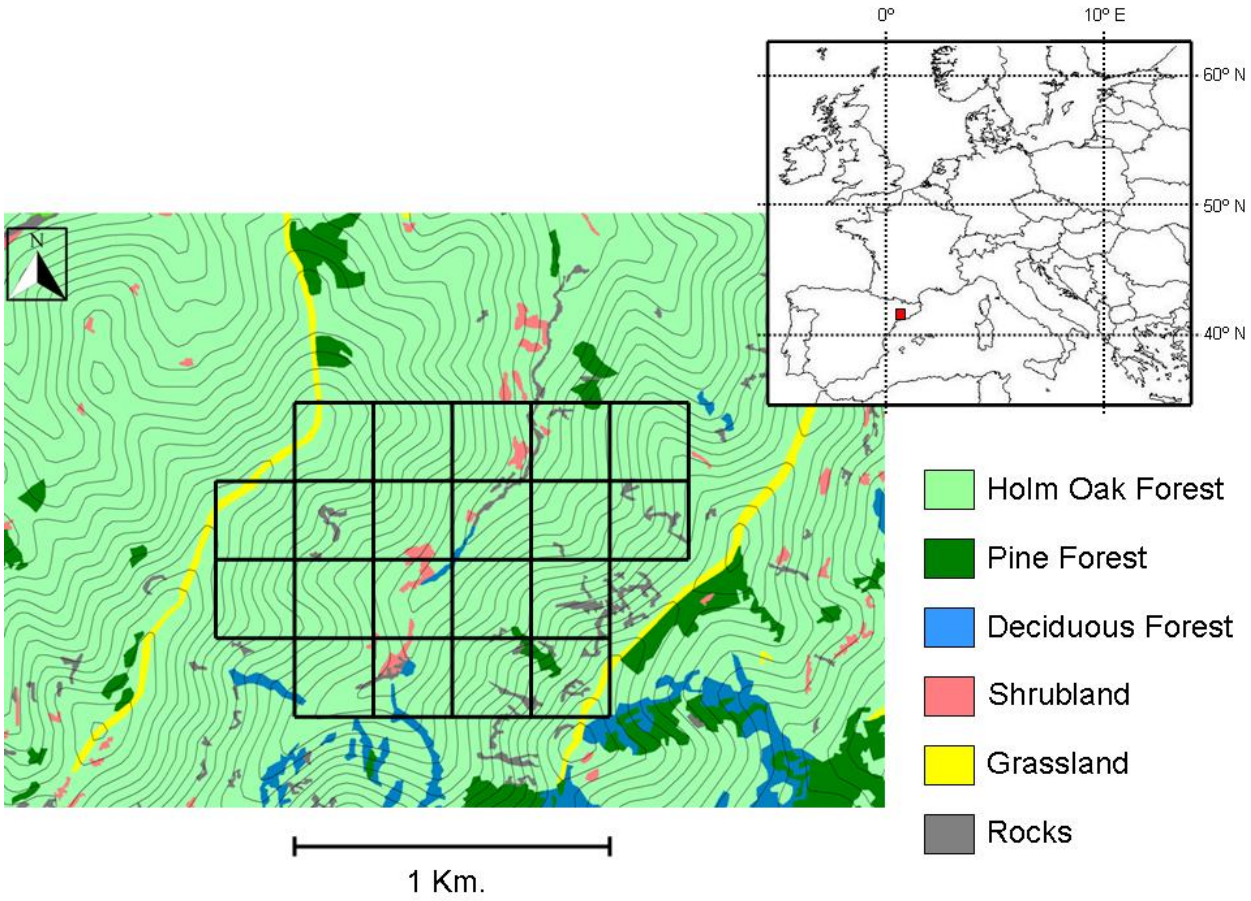
0°
10° E
60° N
50° N
40° N
N
Holm Oak Forest
Pine Forest
Deciduous Forest
Shrubland
Grassland
Rocks
1 Km.

Fig. 1

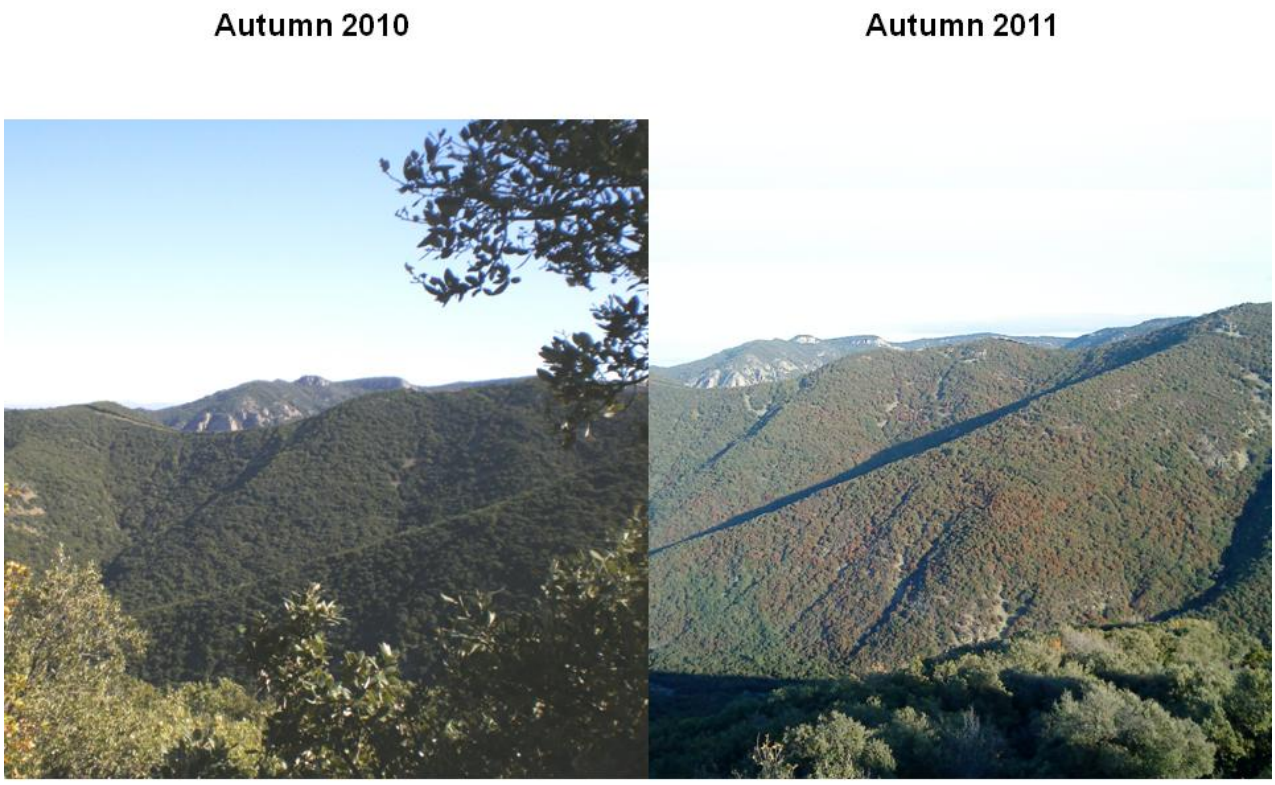

Fig. 2

530

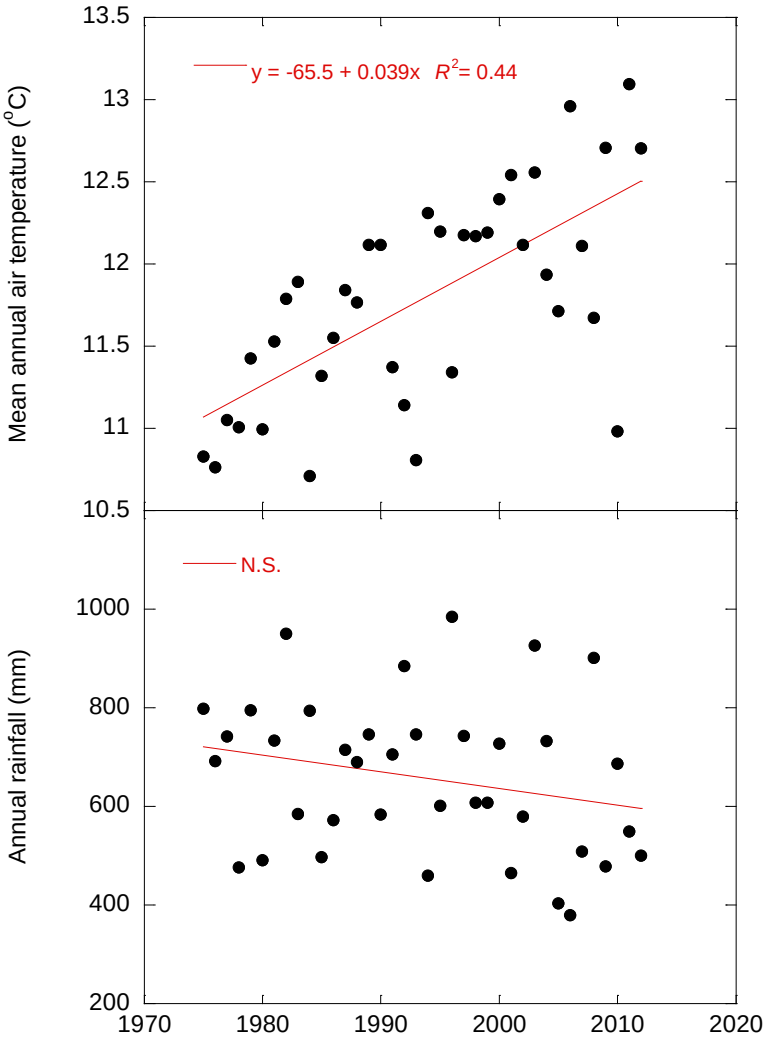

531

532

533

534

535 Fig. 3

536

537

538

539

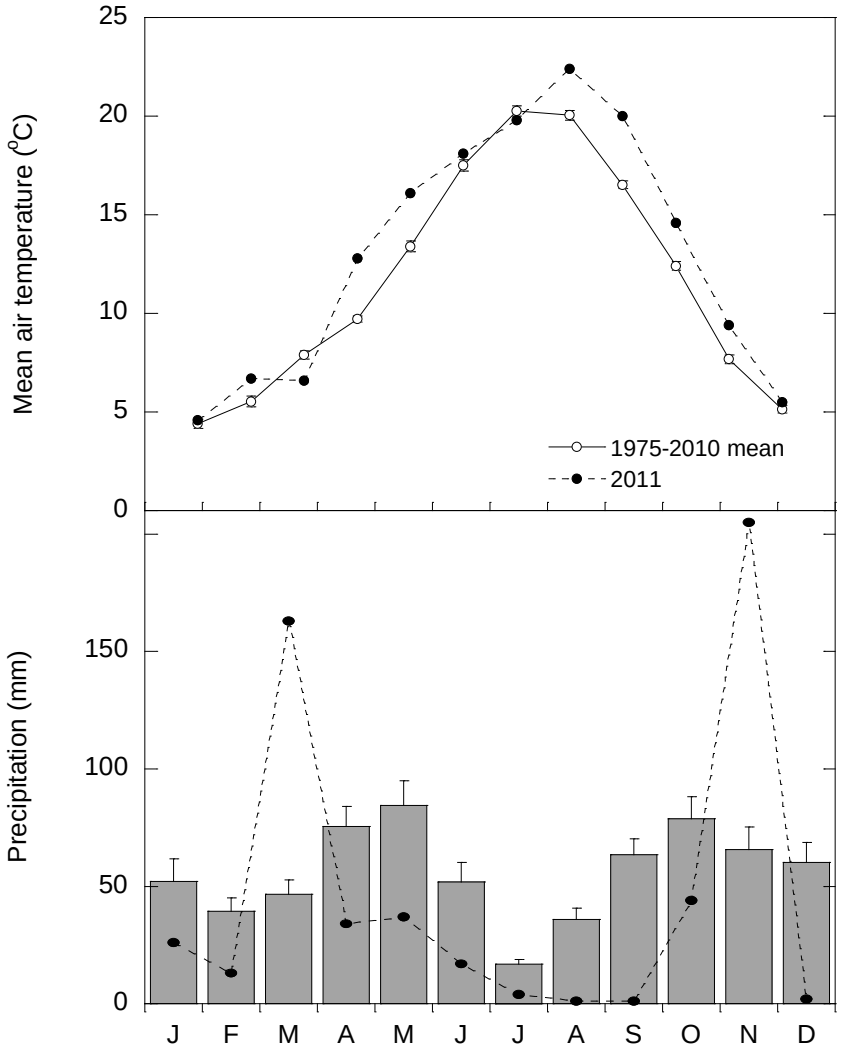

540

541 Fig. 4

542

543

544

545

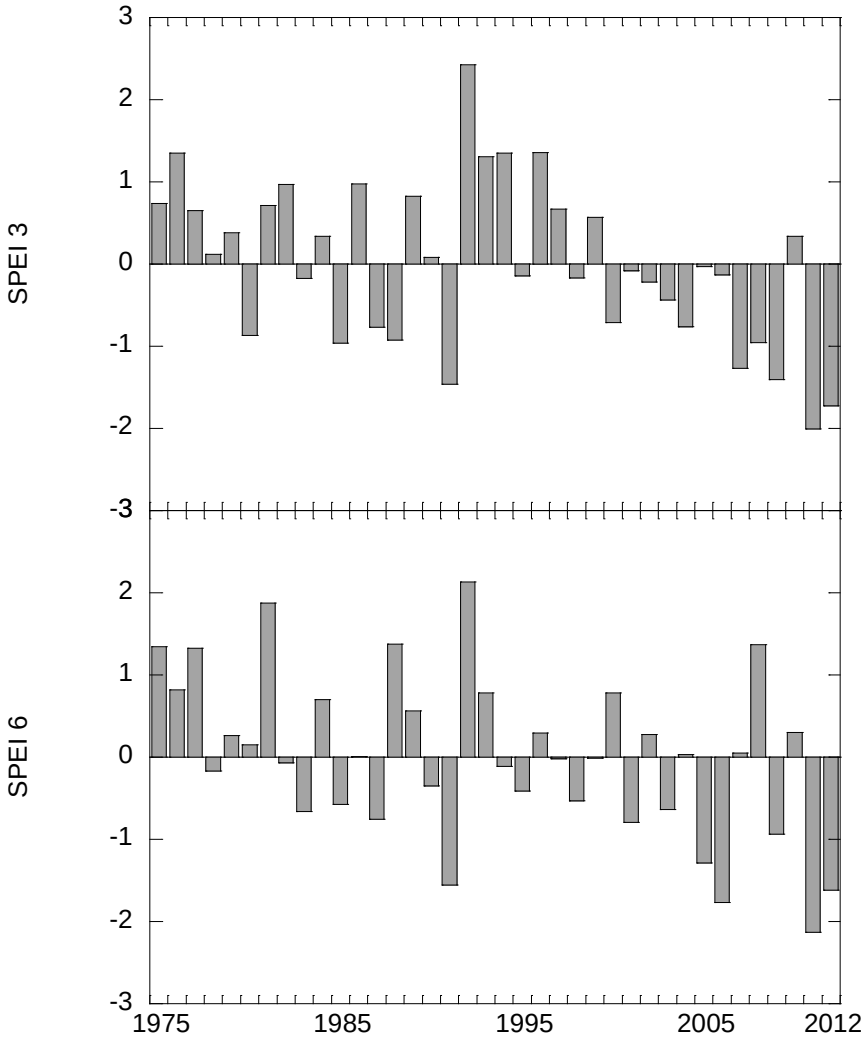

546

547 Fig. 5

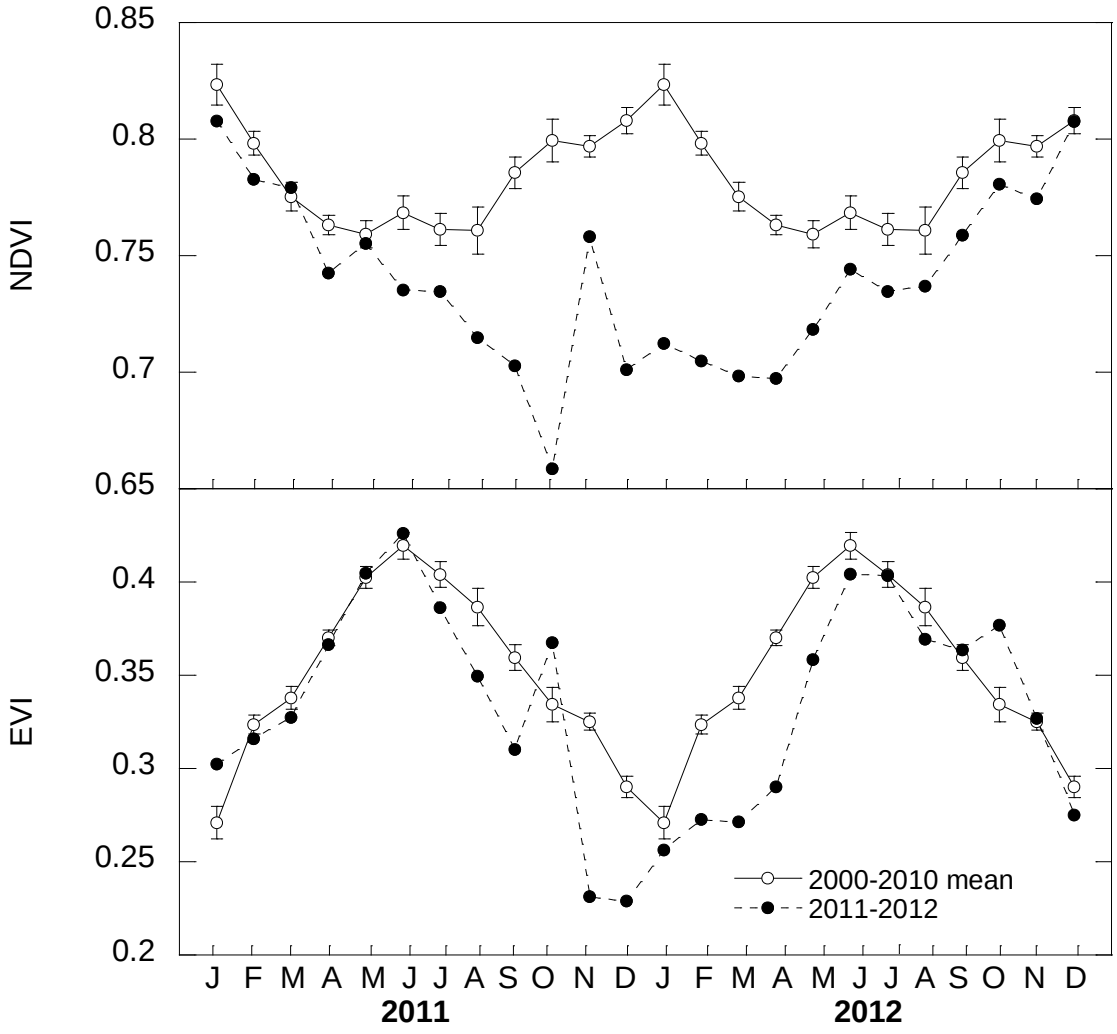
NDVI
EVI
0.85
0.8
0.75
0.7
0.65
0.4
0.35
0.3
0.25
0.2
2000-2010 mean
2011-2012
J F M A M J J A S O N D J F M A M J J A S O N D
2011
2012

Fig. 6

559

560

561

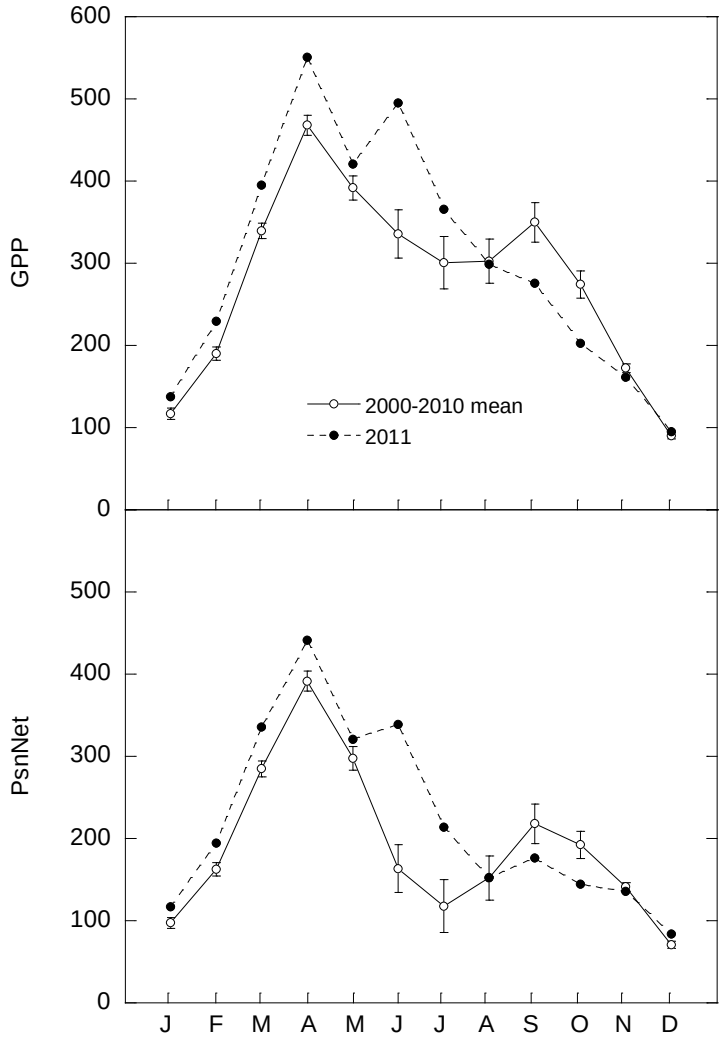

562

563

564 Fig. 7

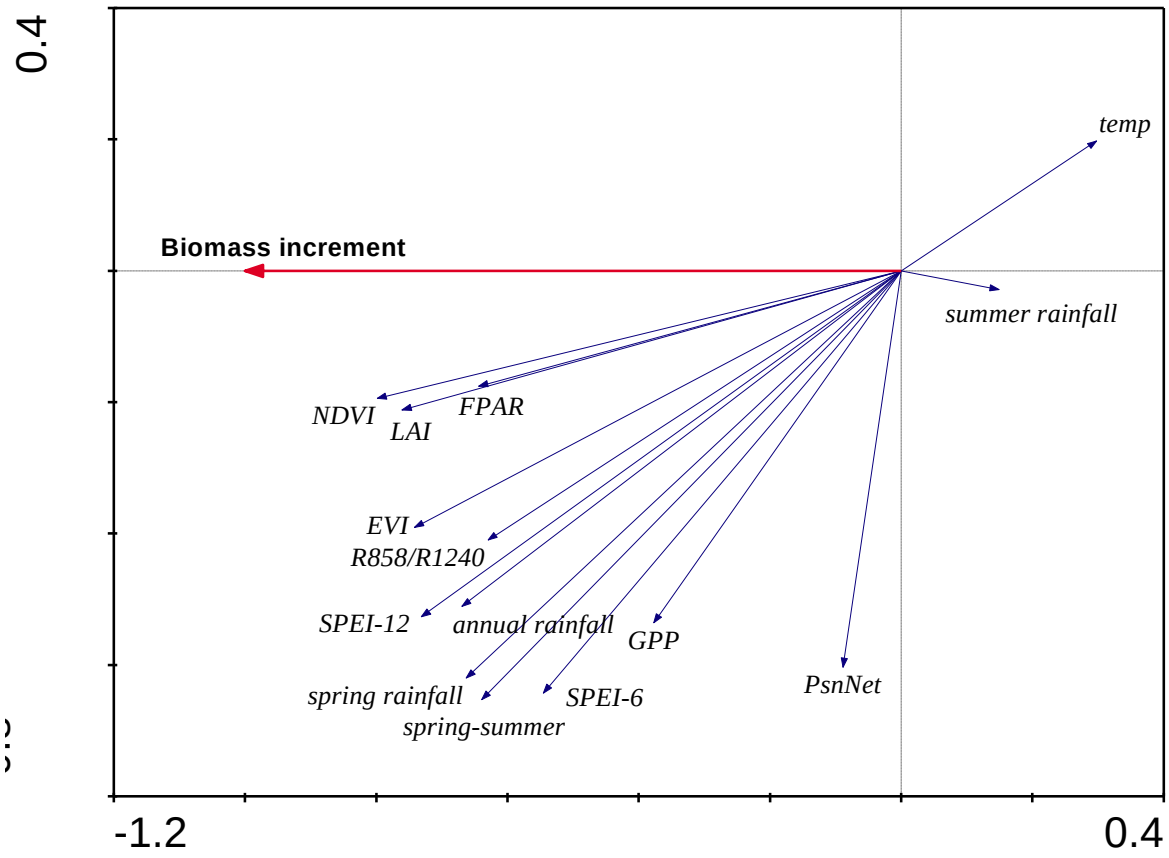
0.4
temp
Biomass increment
summer rainfall
NDVI
LAI
FPAR
EVI
R858/R1240
SPEI-12
annual rainfall
GPP
spring rainfall
SPEI-6
PsnNet
spring-summer
-1.2
0.4

Fig. 8

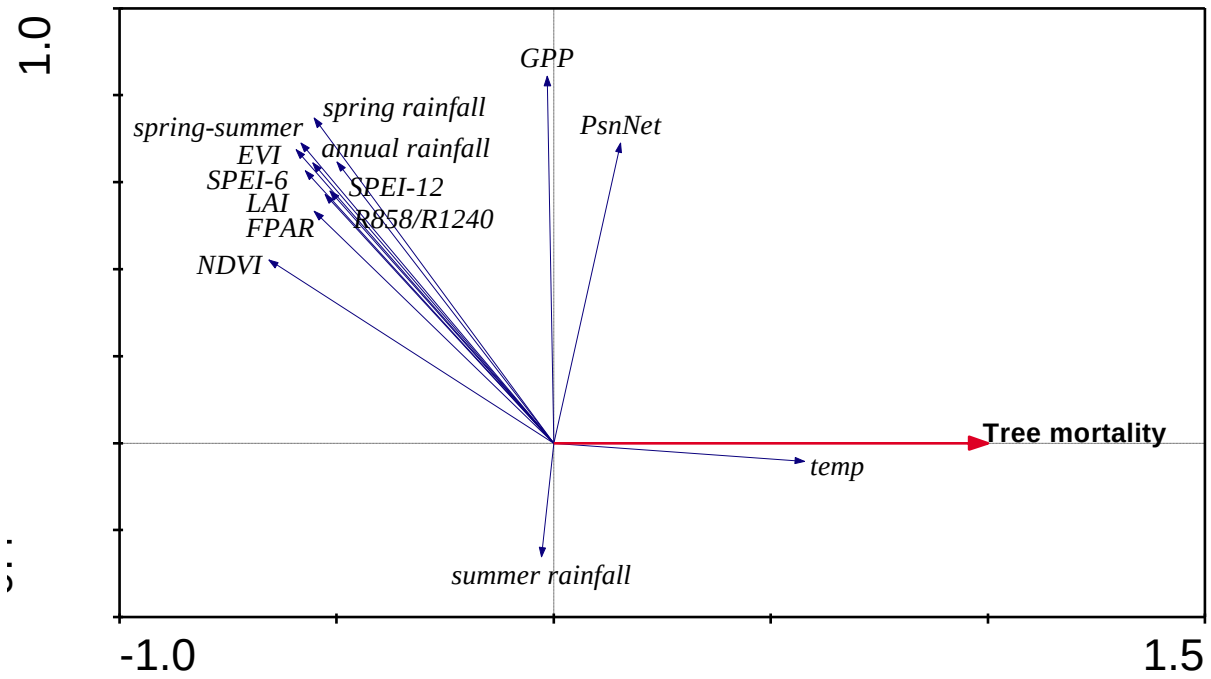
1.0
GPP
spring rainfall
spring-summer
PsnNet
EVI
annual rainfall
SPEI-6
SPEI-12
LAI
R858/R1240
FPAR
NDVI
Tree mortality
temp
summer rainfall
-1.0
1.5

Fig. 9